

3D shape-sensor based on integrated optics in ultra-thin glass

Jannis Koch^{*a,b}, Adrian Droste^{a,b}, Martin Angelmahr^a, Günter Flachenecker^a, Wolfgang Schade^{a,b}

^aDepartment of Fiber Optical Sensor Systems, Fraunhofer Heinrich-Hertz-Institute, Am Stollen 19 H, Goslar 38640, Germany; ^bDepartment of Applied Photonics, Institute of Energy Research and Physical Technologies, Clausthal University of Technology, Am Stollen 19 H, Goslar 38640, Germany

ABSTRACT

3D shape sensors find important applications in industries, e.g. structural health monitoring and medical technology. (Fiber-)Optical shape sensors possess various advantages such as miniature size, high sensitivity and low costs. Current challenges are the necessary increase of stability and reproducibility and the lack of application cases. We present a 3D shape sensor based on an ultra-thin glass (100 μm) approach which allows both a stable and reproducible measurement. The 3D shape sensor presented here is part of the development of a novel and flexible X-ray detector, which serves as a practical application. Femtosecond laser pulses are used for the optical integration of both light waveguides and Bragg gratings into the ultra-thin glass. Bragg gratings serve as strain and ultimately curvature sensors (0 to 20/m) as they are integrated parallel to the neutral bending axis (20-30 μm). The Bragg gratings are organized in a bi-directional network at known positions as all Bragg gratings can be integrated in a single step. The 3D shape sensor has to be calibrated only a single time as it can be mounted on and removed from surfaces without the need of a direct adhesion, resulting in easier integration and higher reproducibility as the neutral bending axis is not moved. A 3D reconstruction algorithm provides a 3D point cloud, which allows the calculation of the shape of the surface (here the detector surface). As the positions of Bragg gratings are well known, a more precise 3D shape recalculation is possible compared to fiber Bragg gratings.

Keywords: curvature sensor, 3D shape sensor, laser materials processing, thin glass, rapid prototyping

1. INTRODUCTION

3D shape sensors are, among others, used in sectors such as the monitoring of structural health and medicinal technology. One way to realize such sensors is to use (fiber-)optical methods which offer the advantages¹ of a small size, high sensitivity, low cost, and the immunity to electromagnetic interferences. 3D shape sensors with glass fibers with Bragg gratings embedded in flexible materials have been realized^{2,3} and also shape sensors directly integrated in polymers are possible⁴. The drawbacks of 3D shape-sensors based on (fiber-)optical bend and curvature sensors are the lack of stability, reproducibility and application cases¹. We present the use of ultra-thin glass as a material for both the substrate and the sensors. Using laser processing, Bragg gratings for curvature measurement can be integrated into ultra-thin glass in a precise manner. The monolithic character of the aluminosilicate glass ensures reproducible measurements as the neutral bending line is not changed when applied to a surface. The FleX-RAY project for novel, flexible X-ray detectors requires the use a non-electrical 3D shape sensor to determine the shape of the X-ray detector.

*jannis.koch@hhi.fraunhofer.de

2. METHODS

2.1 Sensor Concept

The pure bending model⁵ describes the behavior of bent beams. One requirement is that the material must be homogenous or isotropic in elasticity, so the model is not applicable to compound materials which possess different mechanical properties. In the case of ultra-thin glass (AS87eco by Schott), the sensor elements are integrated using femtosecond laser pulses which changes the mechanical properties only negligibly. The refractive index of waveguide and Bragg grating are marginally larger than the substrate or cladding material and therefore the ultra-thin glass curvature sensor can be treated as homogenous and the pure bending model can be applied.

When such beam is under load, the plane inside the beam which experiences no load is also the plane of symmetry for homogenous materials. Compression and stretching are present only above and below the plane of symmetry, further called “neutral bending line” for two-dimensional representations.

A Bragg grating reflects wavelengths λ_B according to the Bragg formula

$$\lambda_B = 2 n_{eff} m \Lambda, \quad (1)$$

where n_{eff} , m , and Λ are the effective refractive index, the reflection order, and the grating distance, respectively.

Bending the beam leads to a compression of the Bragg grating for a positive curvature and to stretching for a negative curvature. Upon compression, the grating distance is reduced and the effective refractive index increases whereas for stretching, the grating points lie farther apart from one another and the effective refractive index shrinks. As the grating distance is affected much more than the effective refractive index, the Bragg wavelength change can be estimated from the bending of the material. A change of temperature also affects both the grating distance and the effective refractive index but is not in the scope of this work as a constant temperature was maintained during the experiments.

In Figure 1, the concept of bending is shown as a cross section for the ultra-thin glass with waveguide and Bragg grating. The waveguide and the Bragg grating are positioned parallel to the neutral bending line in Figure 1a. The side length of the ultra-thin glass is 50 mm with a thickness of 100 μm and the length L_{FBG} of the Bragg grating is 5 mm. The distance y between the Bragg grating and the neutral bending line is 23 μm . When negative bending of radius R from the perspective of the Bragg grating is performed, the situation shown in Figure 1b is obtained. In this case, the Bragg grating is stretched by

$$\Delta L = \frac{L_{FBG}}{R + y} * y. \quad (2)$$

When $R \gg y$, the radius or its inverted, curvature C , can be approximated to be the same for both the neutral bending line and the Bragg grating, yielding

$$\Delta L = \frac{L_{FBG}}{r} * y = L_{FBG} * C * y. \quad (3)$$

When the Bragg grating is compressed, the distance between the grating points Λ shrinks. At the same time, the refractive index is increased but this effect is small enough to be neglected for estimating wavelength shifts under bending. As the wavelength of reflected light is proportional to the grating distance, the wavelength shift can be estimated through

$$\Delta \lambda_B = \lambda_B * C * y. \quad (4)$$

The curvature C can be calculated from the wavelength shift either through a calibration for different curvatures or through the determination of the distance y . The size of y determines the sensitivity of the sensor.

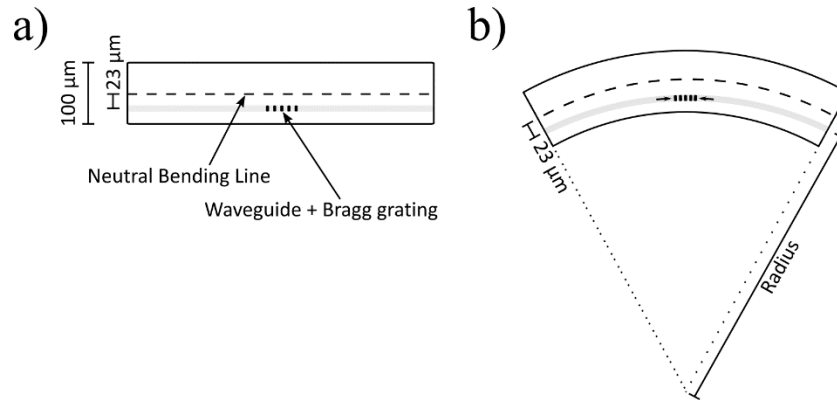


Figure 1. Pure bending model. a) Both waveguide and Bragg grating are positioned parallel to the neutral bending line. b) Under (positive) bending, the Bragg grating is compressed.

2.2 Fabrication

For a thin substrate, we chose 100 μm -thick aluminosilicate glass (Schott AG, AS87eco, refractive index $n = 1.504$) with side lengths of 50 mm, which stands out due to its high flexibility and low thickness. We used a regeneratively amplified Ti:Sa femtosecond laser (Spectra Physics, Tsunami/Spitfire, wavelength: 800 nm, repetition rate: 5 kHz, pulse duration: 100 fs) to integrate both a waveguide and a Bragg grating into the thin glass substrate. After transferring the laser beam into circular polarization and attenuating the energy down to 7.04 μJ , the laser beam is partly cut off by a slit and is subsequently transmitted through a microscope objective (Zeiss, LD Plan-NEOFLUAR 20x/0.4) which focuses the beam 27 μm or 73 μm (23 μm off the midpoint) deep into the glass substrate. The glass substrate is mounted on an air-bearing axis (PI, PIglide A-110). Because of the cutoff at the slit, the beam focus and therefore interaction volume between beam and glass are circular⁶. The beam-glass interaction leads to a positive refractive index change of the glass inside the interaction volume. To create light waveguides, the sample is moved perpendicularly to the laser beam at a speed of 2 mm/s. Eight waveguides were integrated, four above and four below the middle. The waveguides were positioned equidistantly along the sides of the glass. Using a laser scanning microscope, the waveguide depth was determined to be 23 μm off the neutral bending line. For curvature sensing elements, four 5 mm-long plane-by-plane⁷ Bragg gratings are inscribed along each waveguide equidistantly with the same setup and the same slit opening at a pulse energy of 7.41 μJ . In Figure 2, the ultra-thin glass is shown with glass fibers and the positions of the Bragg gratings are indicated.

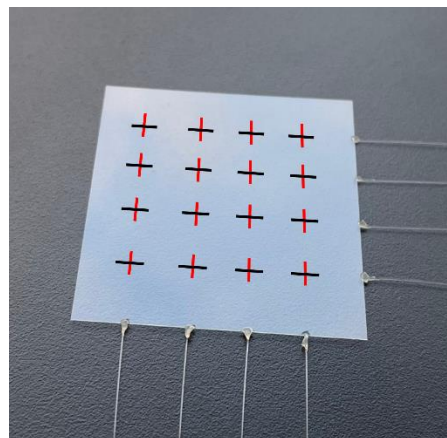


Figure 2. Ultra-thin glass with bi-directional sensor array. Four waveguides in both direction with four Bragg gratings each are indicated (black: x-direction, red: y-direction). A glass fiber is connected to each waveguide for sensor readout.

To interrogate the Bragg gratings, fiber pigtailed (Fibercore, 800 nm, 5.6 μm) were put in proximity to the waveguide facets. At the other end, the fiber pig tails were connected to an interrogation system consisting of a broadband light source

(SUPERLUM, FSLD-840-20-FC), a spectrometer (Ocean Insight, OceanFX), and a polarization randomizer. The polarization randomizer enables a polarization-independent monitoring of the Bragg wavelength shifts and consists of a half-waveplate and a quarter-waveplate rotating in opposite directions. A transparent UV-curing adhesive (Dymax, OP-4-20632-GEL, glass transition temperature at 79 °C) was added between fiber and waveguide, the fiber position was optimized for best Bragg reflection signals and the adhesive was cured by UV light.

2.3 Measurement Principle

For Bragg wavelength probing, the interrogation system from section 2.2 is used. A Gaussian fit is applied to the acquired Bragg wavelengths for peak detection.

To measure the sensitivity of the curvature sensor, the sensor was mounted on a 3D-printed cylinders with curvatures of 0 m^{-1} , 5 m^{-1} , 10 m^{-1} , 15 m^{-1} , and 20 m^{-1} (Figure 3a). 20 m^{-1} corresponds to a radius of 50 mm.

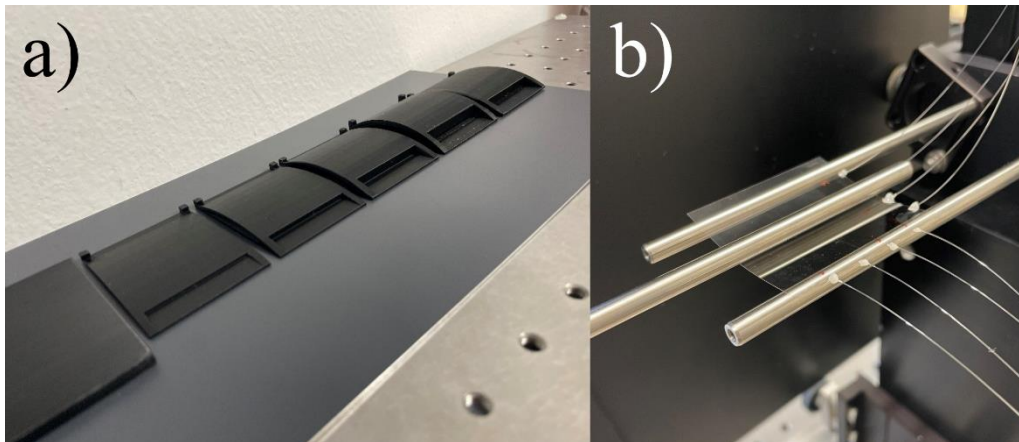


Figure 3. Measurement setups. a) 3D-printed cylinders with curvatures of 0 m^{-1} , 5 m^{-1} , 10 m^{-1} , 15 m^{-1} , 20 m^{-1} , and 17.1 m^{-1} . b) Three-point bending setup.

The wavelength shifts are then compared to the curvatures, which give the sensitivities of the Bragg gratings. From detaching and remounting the sensor onto the cylinder, the remounting repeatability can be obtained.

To determine the linearity of the sensor and the precision or repeatability of measurements when the sensor stays mounted, the curvature sensor is put in a three-point bending setup (see Figure 3b). The bending setup consists of three posts (6 mm diameter) of which the outer two are fixed at a distance of 42 mm and the middle one can be moved with a linear stage (OWIS, LIMES 120-200-MSM), which allows a precise and reproducible change of bending.

2.4 3D-Shape Calculation

The curvatures of all four Bragg gratings along one waveguide were used to create a curve through extra- and interpolation². In this approach, the curvature of each Bragg grating is assumed for the length in which it resides up to the midpoint to the adjacent Bragg grating or the end of the sample. At their intersection, the curves of two Bragg gratings are on the same tangent line.

To move from a two-dimensional representation of a waveguide to a three-dimensional shape consisting of all Bragg gratings from all waveguides, the requirements⁸ were assumed that one side of the sample is fixed in a straight line and that the middle line along the bent direction experiences no effect of torsion.

3. RESULTS AND DISCUSSION

The spectrum of reflected Bragg signals (Figure 4a) shows four peaks corresponding to the four Bragg gratings within one waveguide. The intensity decreases with each next signal due to the attenuation of the waveguide (0.47 dB/cm).

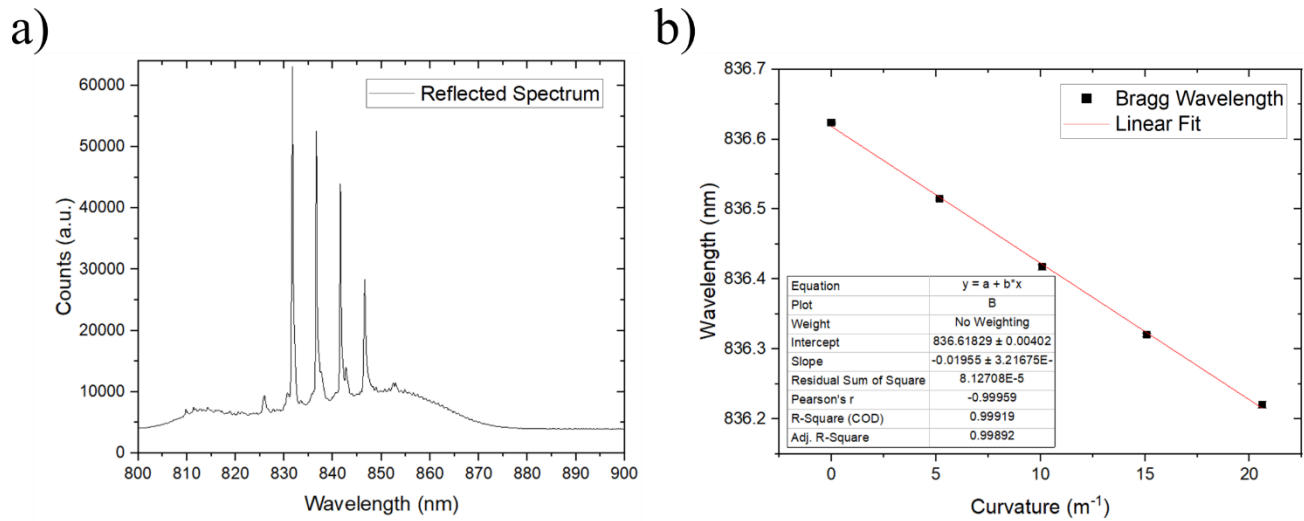


Figure 4. a) Spectrum of reflected Bragg signals in one waveguide. b) Calibration measurement with linear fit of one Bragg grating. Error bars are smaller than the measurement symbols.

To identify the relationship between Bragg wavelength shifts and curvature, the thin-glass sensor was placed on the cylinders shown in Figure 3a with curvatures from 0 m^{-1} to 20 m^{-1} in increments of 5 m^{-1} . The spectra are recorded with an integration time of $5 \mu\text{s}$ and averaged over 20 measurements. This measurement was done for negative and positive bending in both x- and y-direction. The five-point calibrations of all sensors show an average sensitivity of -17.8 pm/m^{-1} .

When remounting the curvature sensor onto the cylinder, a standard deviation of 2.6 pm is measured which corresponds to an error of 0.15 m^{-1} for a sensitivity of 17.8 pm/m^{-1} . The measurements were recorded in an oven at a constant temperature to exclude temperature effects. The temperature dependency of the wavelength shift was determined to be 8.3 pm/K .

To determine the linearity and precision of the sensor, an ultra-thin glass with integrated sensors was placed in the three-point bending setup described in Section 2.3 (Figure 3b). Starting from a neutral position, the middle post is moved in incremental steps of 0.100 mm up to a displacement of 4.200 mm . From there, the post was moved backwards to the initial position and the procedure was repeated four more times. For the other direction, the measurement was repeated after turning the sample upside down. Spectra are recorded with an integration time of $5 \mu\text{s}$, then averaged over 20 samples and subsequently a Gaussian fit is applied to determine the central Bragg wavelengths. The Bragg wavelengths and their standard deviations are plotted against the curvature of a Bragg grating for positive bending in Figure 4b. The curvature values were allocated to the displacement values of the middle post by comparing the wavelength shift at 20 m^{-1} . The standard deviations (on average 4.3 pm) are smaller than the symbols shown in the graph. The linear fits are highly linear at an average R-square of 0.995 , so a two-point calibration would suffice.

For testing, the 3D shape-sensor was exposed to a curvature of 17.1 m^{-1} (Figure 3a, in the back). Using the calibration functions, the curvature at each Bragg grating was calculated from the wavelength shifts. When inter- and extrapolating the curvature data of each Bragg grating in the waveguide, the curve in Figure 5a is obtained. The average error for all Bragg gratings is 0.33 m^{-1} or 1.9% as the last Bragg signal (Figure 5a, at $x=15\text{--}30 \text{ mm}$) is affected by the attenuation (Figure 4a) for high curvatures.

Repeating the process (section 2.4) for all Bragg gratings gives the 3D graph in Figure 5b.

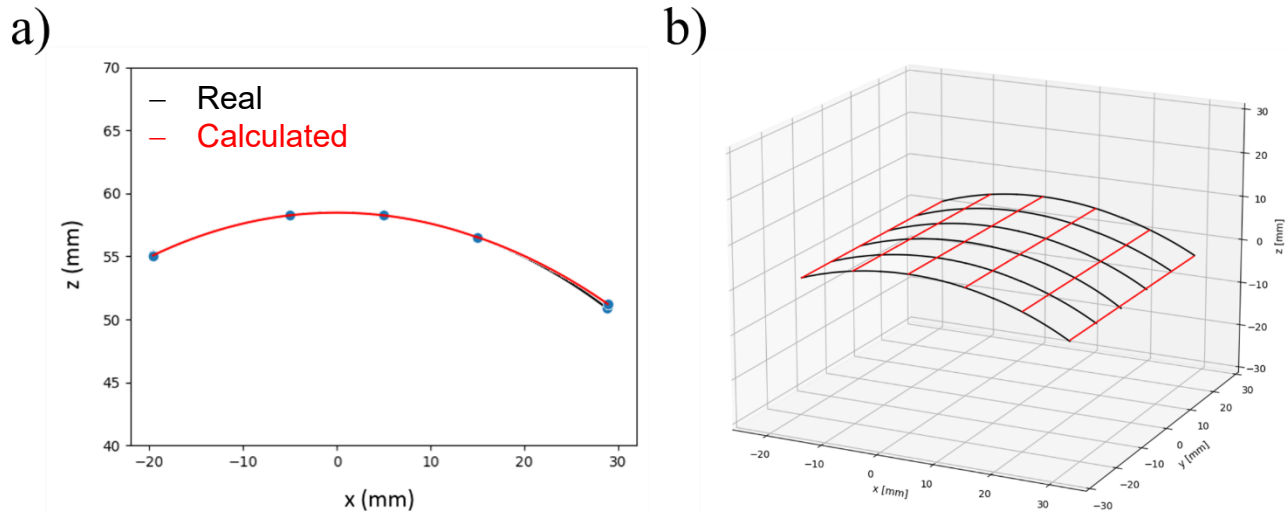


Figure 5. a) Inter- and extrapolation of curvatures along one waveguide. Black: Real curvature. Red: Calculated curvature. b) 3D graph of calculated shape.

4. CONCLUSION

We demonstrated a sensitive and ultra-thin optical 3D shape sensor based on femtosecond laser-processed integrated optics inside ultra-thin glass. Both waveguides and Bragg gratings can be integrated at any desired distance to the neutral bending line which affects the dynamic range of the curvature sensor. An average sensitivity of -17.8 pm/m^{-1} is achieved at a distance of $23 \text{ }\mu\text{m}$ to the neutral bending line with a Bragg wavelength shift. The flexible but monolithic characteristics of thin glass yield a high sensitivity for short distances to the neutral bending line as the pure bending model applied to the ultra-thin glass. The relationship between wavelength shift and curvature is highly linear and measurements are reproducible when remounting the sensor on the same surface. The high linearity makes a two-point calibration sufficient and the sensor does not have to be recalibrated as the neutral bending line is not moved when the glass is mounted on a surface. The curvatures of the Bragg gratings can be used to calculate curves along a waveguide and ultimately calculate a 3D shape when a bi-directional network of curvature sensors is used. Altering the thickness of the glass, either a thinner sensor ($< 100 \text{ }\mu\text{m}$) or a more sensitive sensor can be manufactured when the distance between Bragg grating and neutral bending line is increased. For the application as a surface shape monitoring device within the Flex-RAY project, the actual shape of the active area of the X-ray detector has to be determined from the calculated shape of the ultra-thin sensor, which we plan to do in the near future. Also, an easy and practical way of mounting the sensor for the layperson still has to be identified. A 3D shape sensor in ultra-thin glass poses a good alternative to existing (fiber-)optical shape sensors.

ACKNOWLEDGMENT

This project has received funding from the European Union's Horizon 2020 Research and Innovation Program under grant agreement No. 899634.

REFERENCES

- [1] Wang, Q., Lui, Y., "Review of optical bending/curvature sensor," *Measurement* 130, 161-176 (2018).
- [2] Xu, L., Ge, J., Patel, J., et. al., "Dual-layer orthogonal fiber Bragg grating mesh based soft sensor for 3-dimensional shape sensing," *Opt. Express* 25(20), 24727-24734 (2017).

- [3] Lun, T., Wang, K., Ho, J., "Real-Time Surface Shape Sensing for Soft and Flexible Structures Using Fiber Bragg Gratings," *IEEE Robot. Autom. Lett.*, 4(2), 1454-1461 (2019).
- [4] Rosenberger, M., Pauer, H., Girschikofsky, M., et. al., "Flexible Polymer Shape Sensor Based on Planar Waveguide Bragg Gratings," *IEEE Photon. Technol. Lett.*, 28(17), 1898-1901 (2016).
- [5] Boresi, A. P., Schmitt, R. J., Sidebottom, O. M., [Advanced Mechanics of Materials], John Wiley & Sons, Inc., New York, Chichester, Brisbane, Toronto & Singapore, 5-10 (1993).
- [6] Spence, D., Marshall, G., Ams, M., et. al., "Slit beam shaping method for femtosecond laser direct-write fabrication of symmetric waveguides in bulk glass," *Opt. Express* 13(15), 5676-5681 (2005).
- [7] Lu, P., Mihailov, S., Ding, H., et. al., "Plane-by-Plane Inscription of Grating Structures in Optical Fibers," *J. Light. Technol.* 36(4), 926-931 (2018).
- [8] Zhang, H., Zhu, X., Gao, Z., et. al., "Fiber Bragg grating plate structure shape reconstruction algorithm based on orthogonal curve net," *J. Intel. Mater. Syst. Struct.* 27(17), 2416-2425 (2016).